MNRAS **000**, 1–8 (2019) Preprint 10 February 2020 Compiled using MNRAS LATEX style file v3.0

Orbital dynamics of highly probable but rare Orionid outbursts possibly observed by the ancient Maya

J. H. Kinsman[1]★ and D. J. Asher[2]†
[1]*P.O. Box 723, Murrayville, Ga, 30564, USA*
[2]*Armagh Observatory & Planetarium, College Hill, Armagh BT61 9DG, UK*

Accepted XXX. Received YYY; in original form ZZZ

ABSTRACT

Using orbital integrations of particles ejected from Comet Halley's passages between 1404 BC and 240 BC, the authors investigate possible outbursts of the Orionids (twin shower of the Eta Aquariids) that may have been observed in the western hemisphere. In an earlier orbital integration study the authors determined there was a high probability linking probable outbursts of the Eta Aquariid meteor shower with certain events recorded in inscriptions during the Maya Classic Period, AD 250–900. This prior examination was the first scientific inquiry of its kind into ancient meteor outbursts possibly recorded in the western hemisphere where previously no pre-Columbian observations had existed. In the current paper the aim is to describe orbital dynamics of rare but probable Orionid outbursts that would have occurred on or near applicable dates recorded in the Classic Maya inscriptions. Specifically, significant probable outbursts are found in AD 417 and 585 out of 30 possible target years. The driving mechanisms for outbursts in those two years are Jovian 1:6 and 1:7 mean motion resonances acting to maintain compact structures within the Orionid stream for over 1 kyr. Furthermore, an Orionid outburst in AD 585 recorded by China is confirmed.

Key words: celestial mechanics – comets: individual: 1P/Halley – meteorites, meteors, meteoroids

1 INTRODUCTION: HALLEY'S COMET AND ORIONIDS

Comet 1P/Halley's meteoroid stream produces twin showers: the Orionids (IAU meteor shower 008 ORI) at the ascending node and the Eta Aquariids (031 ETA) at the descending node. The authors' previous investigations (Kinsman & Asher 2017) focused on the Eta Aquariid outbursts because the heliocentric distance of the descending node of the parent comet was approximately equal to the Earth's orbital radius near the middle of the Maya Classic Period (i.e., ~AD 530). In contrast, the present paper's investigations focus on the Orionids in spite of the fact that the ascending node of Halley was nowhere near Earth's orbital radius by the Maya Classic time (AD 250–900).

Orionid outbursts during that epoch were likely rather rare as exhibited by the historical record, where China was the only ancient culture to record Orionid outbursts earlier than AD 900, and those were in AD 288 and AD 585. Similarly, in the present paper, the authors found only two probable outbursts out of a database from the Maya corpus of inscriptions[1] that currently contains 30 different viable 'target years' (Sections 2 and 3) prior to AD 900. With such a small sample size, the authors' goal is not to correlate events in the Maya record to these two probable outbursts as in their previous study, but to analyze the orbital dynamics of the outbursts themselves. The year 585 was not only recorded in the Chinese annals, but remarkably was also found as one of the two years in which a probable Orionid outburst could have been observed by the Maya.

★ E-mail: jhkinsman@gatech.edu
† E-mail: David.Asher@armagh.ac.uk

[1] Of all the ancient cultures found in the western hemisphere, the Maya civilization is the only one with a rich corpus of dates (cf. Kinsman & Asher 2017, sec. 1.1) available for investigation. As stated in the authors' previous study (Kinsman & Asher 2017), currently there is no known definitive statement in the Maya corpus of a 'shooting star' or meteor shower. The authors rely on the most recent correlation literature for converting Maya calendar dates into the Julian dates of the Christian calendar, the Martin-Skidmore correlation constant (Martin & Skidmore 2012), and the most recent carbon dating (Kennett et al. 2013).

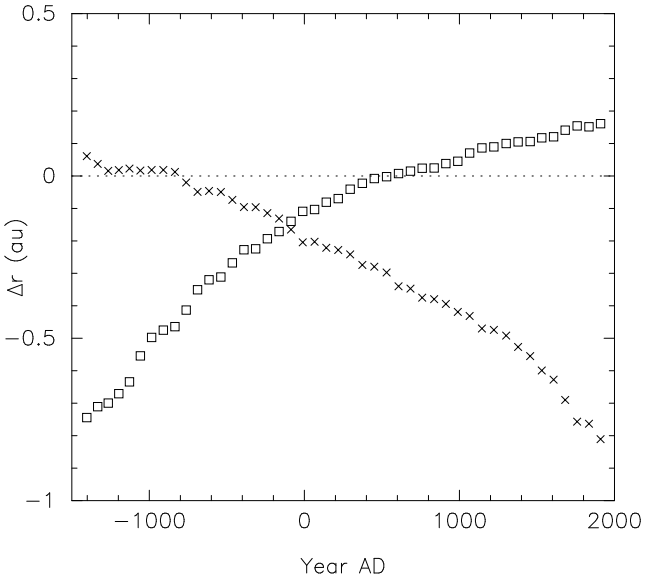

Figure 1. Distance of Earth orbit from comet nodes at perihelion returns of 1P/Halley listed by Yeomans & Kiang (1981). Squares: descending node, corresponding to ETA. Crosses: ascending (ORI). Positive/negative Δr is Earth orbit outside/inside comet orbit.

By the present epoch, the general tendency for particles released ~3 kyr ago is for the Orionid node to have precessed well beyond Earth's orbit (Ryabova 2003, fig. 6). Sato & Watanabe (2007), however, demonstrated that there are observable Orionid outbursts even in the present epoch resulting from particles released 3 kyr ago and trapped in a Jovian 1:6 resonance, raising the possibility that owing to a similar dynamical effect Orionid outbursts could have occurred in the first millennium AD.

Thus given those present epoch Orionid outbursts, it is remarkable that the last time Halley's ascending node was equal to the Earth's orbital radius was approximately 800 BC (Fig. 1). Thereafter the node continued to precess further outside Earth's orbit. For a number of centuries prior to 800 BC, however, the ascending nodal distance maintained a constant value around 0.98 au from about 1266 BC until about 836 BC, sustaining very little precession. Figure 1 shows that for particles ejected around 1000 BC the precession rate must be slowed almost to nothing if Orionid intersections are to occur during either the Maya Classic Period or the present epoch, whereas the ascending node of Halley itself has moved a few × 0.1 au outside Earth in the Classic and several × 0.1 au outside at present. The precession rate of angular orbital elements of meteoroid stream particles can be dramatically affected by resonances (Froeschlé & Scholl 1986; Scholl & Froeschlé 1988; Froeschlé & Froeschlé 1992; Asher & Clube 1993). In Section 4 we shall see that Orionid outbursts occur – i.e., ascending nodes are Earth intersecting – during the Maya Classic Period due to particles trapped in resonance since release from Halley at its 1266 BC and 911 BC returns. The large tightly clustered segments of particles in Jovian resonances actually impeded the precession of the meteoroid trails.

Sekhar & Asher (2014) verified historical outbursts in the AD 1400's and 1900's and reported that Halley was trapped in a 1:6 resonance with Jupiter from 1404 BC to 690 BC. The two conditions of Halley's ascending node being very close to Earth and Halley being in a strong resonance with Jupiter for over seven centuries set up a unique situation: particles released from Halley over this long 700 year period could result in particles trapped in resonance that would later impact Earth. Amazingly, the result would be sharp displays of meteor outbursts due to particles released from the comet over a thousand years earlier. Realizing the potential for outbursts during the Maya Classic Period due to resonant trappings added further impetus to investigate Orionid outbursts.

This paper will use orbital dynamics to post-predict accurate dates and times of Orionid outbursts that would have been observable by the ancient Maya civilization, potentially noted by dates recorded in extant inscriptions. Computations using the same dynamical technique successfully match the ancient Chinese records from AD 585.

2 METHODOLOGY

Our methodology for investigating Orionid outbursts was similar to that used with the Eta Aquariid investigations: given a beginning epoch where particles were ejected, we considered target years found in the Maya corpus where those particles would produce a meteor outburst. The authors considered a 'target' year as a year found in the corpus of inscriptions that included a date that fell within a range approximately one week before to approximately two weeks following a typical Orionid shower, with 'typical' taken as spanning a J2000 solar longitude range of 200–208°.

Although over 300 Maya sites (found in the present countries of Mexico, Guatemala, El Salvador, Belize and Honduras) exist with hieroglyphic inscriptions (Prager et al. 2014), only about 150 of these sites contain legible dates (Mathews 2014). Numbering well over 1000 dates, approximately 35 of these fell within our criteria. Given that some of the events related to these dates were unknown or of questionable decipherment, we chose 30 of the remaining candidates from the Mathews database and additional sources for the following entries in Table A1: 1 (Schele & Miller 1986, p.120–121, plate 33); 2,3 (Mathews 2014, dates not certain); 4 (Adams 1999, plate 2,3); 10,17,18 (Stuart & Canuto 2017); 11 (Grube & Martin 2004, p. II-38); 13 (Grube & Martin 2004, p. II-36); 14 (Helmke & Awe 2016); 15 (Grube & Martin 2004, p. II-38); 20 (Stuart et al. 2015); 24 (Martin 2015); 26 (Schele & Freidel 1990, p.325); 27 (Vail & Hernández 2018); 28 (Stuart 2004, noted date is one of three options provided by Stuart); 29 (Grube & Martin 2004, p. II-91); other entries in Table A1 are from Mathews database.

Due to variations in initial orbital period and planetary perturbations, there was little chance of the particles staying together after several revolutions (Plavec 1956, 1957). Therefore, the authors looked for particles that had been trapped in clusters by resonant actions with the larger planets. As the dynamical evolution of particles in a trail released at a given perihelion return of the parent comet depends primarily on the particles' orbital period (Plavec 1956), the 'dust trail model' comprises ejection in tangential directions

to the comet's trajectory at perihelion. As before, the authors adopted the difference, Δa_0, between the semi-major axes at ejection time of the particle, a_0 and of the comet, a_c to parametrize the trail:

$$\Delta a_0 = a_0 - a_c$$

The solution values of Δa_0 are values where particles reach the node in the target year, close to the target date in that year. The forward integration from the ejection epoch yields quantities f_M, Δr and nodal longitude *in the target year*, corresponding to given Δa_0. The density of the outburst in this dust trail model is determined by a product of terms as follows (cf. Asher 2000, p. 18, eq. 5):

$$f_r(r_E - r_A) f_a(\Delta a_0) f_M$$

where f_r is a function of Δr, the difference between the heliocentric distances of Earth and the particle's ascending node; f_a is a function of Δa_0; and f_M, the *mean anomaly factor* is proportional to the along trail spatial density of particles, measuring how much the particles in the stream stretch out over time. The highest density, i.e., the greatest ZHR occurs when Δr is the smallest (with some activity enhancement for $|\Delta r|$ up to a few $\times$ 0.001 au), Δa_0 is the smallest, and f_M is the largest (typically f_M closest to 1.0 is the highest). Whether or not the meteors are visible to the Maya astronomers depends on the time of day that Earth passes through the ascending nodal longitude of the particles.

A range of 16–22 au in a_0 covers the ejection speeds of particles producing visual meteors, allowing also for the typical change in orbital period due to radiation pressure (Kinsman & Asher 2017). Following similar procedures in the previous analysis, integrations were carried out beginning with 601 particles spaced 0.01 au apart, and further integrations were performed until the particles converged on solution values Δa_0, Δr and f_M showing an outburst at a specific time and date (Kinsman & Asher 2017).

As in Kinsman & Asher (2017), orbits for 1P/Halley's perihelion returns were from Yeomans & Kiang (1981, table 4, orbit well known back to 1404 BC), initial state vectors of eight planets (planetary barycentres) were from JPL Horizons (Giorgini et al. 1996), and the RADAU algorithm (Everhart 1985) was used in the MERCURY integrator (Chambers 1999).

3 RESULTS

Integrations were performed for all Halley returns in the 1404 BC to 240 BC range for 30 target years (Table A1) during the Classic Period to find what particles reach the ascending node around ORI time in those years. If those particles' heliocentric distance is near Earth's orbit, they can potentially produce a meteor outburst.

The authors found productive returns[2] for two separate years, AD 417 and 585. In 417 two segments of the same group of particles, trapped in a 1:7 resonance with Jupiter (Sec. 4), likely impacted Earth in rapid succession early in the morning on September 24, likely producing strong meteor displays. Table 1 shows the details of the impact of the particles on that date.

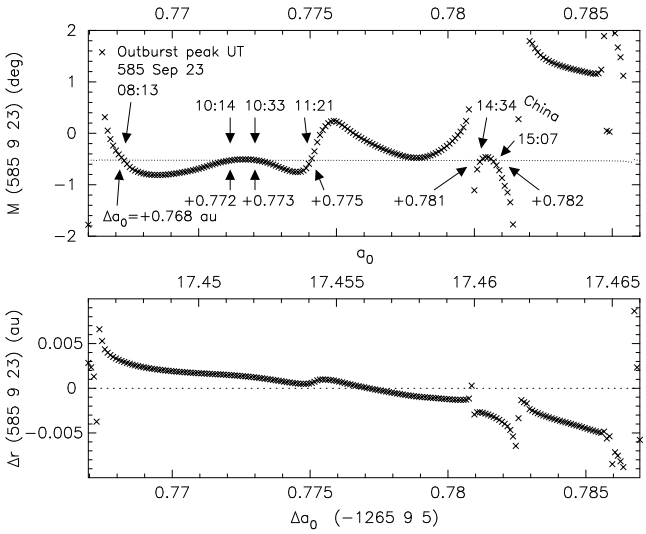

Figure 2. In AD 585, on September 23, a tightly-packed stream of particles crossed the Earth's orbital plane six separate times causing two outbursts visible to China and likely three or four outbursts visible to the Maya. In practice the outbursts from the six distinct trail encounters may overlap somewhat. Particles with $M \approx -0.5°$ on this date are at Orionid node when Earth is nearby.

Both outbursts, peaking within just a few minutes of each other and thus overlapping, were relatively strong with robust mean anomaly factor f_M and fairly close to a central impact with the difference between Earth's orbital radius and the particle stream within $\sim 10^{-3}$ au. The particles were likely medium size in terms of visual meteors, since $\Delta a_0 \approx +1$ au (higher and lower Δa_0 corresponding to smaller and larger meteoroids respectively; McNaught & Asher 1999). Viewing conditions were optimum as the radiant at the computed peak time was about 46° above the eastern horizon and the waning crescent moon, 27.2 days old, was in Virgo and had not risen yet. Five days following the probable outburst on September 24 the birth of an unknown ruler was recorded on 417 September 29.

In addition to the results from 417, the authors found that strong Orionid outbursts occurred in 585 on September 23 due to a resonant cluster of particles. The first segment would have been visible to the Maya and the latter of that same cluster was visible to the Chinese later that same day (Table 2). These meteoroid-sized particles were from the 1266 BC Halley passage, trapped in a 1:6 resonance with the planet Jupiter (Sec. 4).

Figure 2 shows how this cluster of particles provides outbursts on September 23 starting at 08:13 UT (02:13 AM local Maya time) and ending at 15:07 UT (10:07 PM local Daxing, China time), the first four outbursts occurring when the Orionid radiant is above the horizon during hours of darkness for the Maya (the fourth occurs 25 minutes before sunrise at 11:21), while the last two occurred at 14:34 and 15:07 UT, during hours of darkness in China. The fact that the authors' results coincided with the actual observation from China, and that remarkably both outbursts originated

[2] Additional weak returns were found for the years 630, 634, 648 and 714, however any activity would likely have produced only a slightly enhanced display of the shower if at all and not a quantifiable outburst.

Table 1. A strong Orionid outburst likely occurred on AD 417 September 24 due to meteoroid-sized particles from 1P/Halley in 911 BC trapped in 1:7 resonance with Jupiter. First two columns: perihelion return of comet when particles released into trail; semi-major axis difference from comet at that time. Remaining columns are trail's Earth encounter in 417: solar longitude; date (Julian calendar); time (UT); trail centre's nominal miss distance; f_M (stretching factor along trail); visibility from Maya longitudes.

Trail	Δa_0 (au)	$\lambda_\odot$ (J2000)	Date	Time	Δr (au)	f_M	Vis
911 BC	+1.183	204°.057	Sep 24	06:36	+0.00110	−0.016	yes
911 BC	+1.175	204°.094	Sep 24	07:30	−0.00102	−0.146	yes
911 BC	+1.180	204°.100	Sep 24	07:37	−0.00116	+0.392	yes

Table 2. Orionid outbursts in AD 585 September resulting from the 1P/Halley 911 BC (1:7 resonance) and 1266 BC trails (1:6 resonance), recorded by China and possibly observed by the Maya. +5m in the Vis column indicates the outburst occurred 5 minutes after the end of the referenced visual observation time, i.e. 25 minutes before sunrise, and −5m indicates the outburst occurred 5 minutes prior to radiant rise. For columns cf. Table 1.

Trail	Δa_0 (au)	$\lambda_\odot$ (J2000)	Date	Time	Δr (au)	f_M	Vis	
1266 BC	+0.768	202°.048	Sep 23	08:13	+0.00296	+0.048	vis	Maya
1266 BC	+0.772	202°.131	Sep 23	10:14	+0.00145	−0.388	vis	Maya
1266 BC	+0.773	202°.145	Sep 23	10:33	+0.00120	+0.554	vis	Maya
1266 BC	+0.775	202°.178	Sep 23	11:21	+0.00057	−0.031	+5m	Maya
1266 BC	+0.781	202°.311	Sep 23	14:34	−0.00271	−0.043	−5m	China
1266 BC	+0.782	202°.334	Sep 23	15:07	−0.00315	+0.054	vis	China
911 BC	+1.447	203°.923	Sep 25	05:27	−0.00168	−0.013	vis	Maya
911 BC	+1.343	204°.134	Sep 25	10:33	+0.00105	−0.093	vis	Maya

from nearby resonant segments of the same trail, virtually assures the highest of probabilities regarding the Maya outburst as well as confirming the China observations.

The description of the outburst recorded at China reads: 'several hundred meteors scattered in all directions and came down.' 5th year of the Kaihuang reign period of Emperor Gaozu of the Sui Dynasty, 8th month, day wushen [45]; [Bei shi: Sui Wen di ji] ch. 11. [Sui shu: Gaozu ji] ch. 1. (Pankenier et al. 2008, pp. 313, 650)

Comparing the parameters for the probable Maya outbursts versus the Chinese (Table 2), the outbursts likely seen in the Maya area would have been much more intense than the Chinese display for two reasons–the along trail density $|f_M|$ was around ten times greater than the Chinese, ~0.5 vs ~0.05, and the nominal miss distance $|\Delta r|$ from the Earth was less than half that of the Chinese, 0.0012 vs 0.0027 au.

More Orionid outbursts from the 911 BC trail also occurred two nights later on September 25 that would have been visible to the Maya (Table 2). The particles causing the two outbursts on this date were trapped in a 1:7 resonance, also with Jupiter (Sec. 4).

Following the probable outburst on September 23, fifteen days later on 585 October 8 (Table A1), the ruler of Naranjo celebrated 40 years of rulership.

In the specific results noted in the Tables and the above discussion, we quote nominal trail encounter times to the nearest minute UT, noting that the specific numbers allow comparison of results with other models, not that the numbers are actually accurate to the minute. The integration results regarding the 585 China observations do, however, indicate that Orionid trail encounters can be computed to an accuracy of fractions of the day, i.e., correct observable longitude on Earth's surface. Similarly, present epoch Orionid outbursts due to resonant trails 3 kyr old have been successfully computed (Sato & Watanabe 2007; Sekhar & Asher 2014).

4 MEAN MOTION RESONANCE

4.1 Orbital ratios

Although trails only a few revolutions in age are generally compact enough to produce meteor outbursts, the meteoroids causing the 417 and 585 outbursts were rather older, ~20 revolutions. Here (Sec. 4) we shall see that these meteoroids remained synchronized in an integral orbit-to-orbit ratio with Jupiter, defined as resonance. If Jupiter (or another planet) has a strong gravitational force, particles can stay locked in such a synchrony for a long time, up to thousands of years, and moreover the continuous action of the resonance can allow a cluster of particles to remain compact (Emel'yanenko & Bailey 1996; Emel'yanenko 2001; Jenniskens et al. 2002; Sekhar & Asher 2013; Sekhar et al. 2016). Indeed the salient point of this work unequivocably demonstrates that sharply focused outbursts can occur, in 417 and 585, from these very long-term resonant particles ejected over 1000 years earlier.

Figure 3 shows how a trail of particles, released from Halley during its perihelion passage in 911 BC, by the year 585 has broken up into three main segments of particles with a few smaller segments corresponding to weaker resonances as well as other individual particles scattered chaotically. A plot of the same particles but shown in the year 417 would be similar except the groupings of particles would be shifted vertically. The three main segments indicate particles trapped tightly in resonances with the orbit of Jupiter in the ratio of 1:6, 1:7 and 1:8, left to right respectively.

In a rather rare distribution, both the 1:6 and 1:7 orbital ratios indicate large groupings of particles simultane-

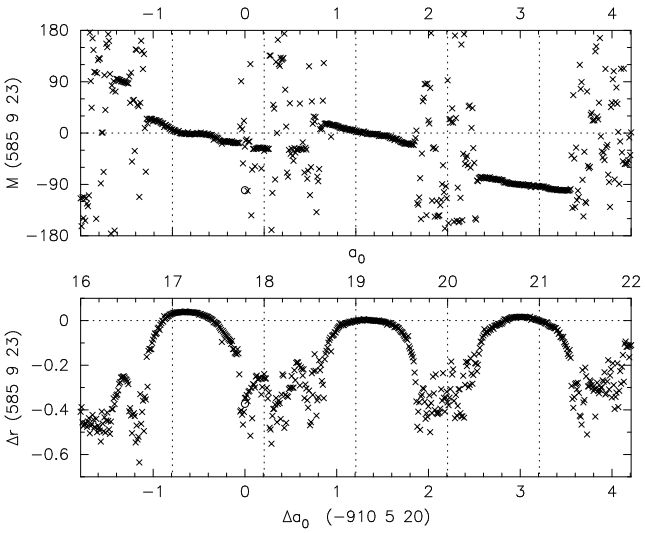

Figure 3. Particles in AD 585 ejected by 1P/Halley in 911 BC over semi-major axis range a_0 = 16 to 22 au. Three major segments of particles are trapped in Jovian resonances (left to right) 1:6, 1:7, and 1:8. Upper panel indicates mean anomaly M (degrees) in 585 September; ascending node is only ~0.5° from perihelion, thus M close to zero is necessary for an Orionid outburst in 585. Lower panel indicates radial distance (au) from Sun, expressed as $\Delta r = r_E - r_A$, thus Δr=0 coincides with Earth. Halley noted by small circle at $a_0 \approx 17.8$ au.

ously at $M \approx 0$ and $\Delta r \approx 0$, setting up potentially very strong outbursts, given the appropriate time of night for visual observation. As we indicated in Section 3, this is indeed the case for the 1:7 resonance (i.e., particles exist with small enough Δr; for the 1:6, on closer examination than can be seen in Fig. 3, particles with exactly suitable M turn out to be a little too distant in Δr). The 1:6 and 1:7 coincidence occurs at this time because AD 585 is close to 126 Jovian periods P_J after 911 BC: both 6 and 7 divide 126. Resonant 1:8 particles are ~$\frac{1}{4}$ revolution (~90° in M) behind.

In actuality, the resonant period differs from the exact integer ratio multiple of P_J (Murray & Dermott 1999, p. 331) (Sekhar & Asher 2014, pp. 54–55). Emel'yanenko (2001, table 1) computes semi-major axes of resonances in several streams and these differ from the nominal resonant semi-major axes a_n which would come from the P_J multiple and Kepler's 3rd Law. However, the difference is slight and for explanatory purposes we neglect it, thus 18 periods of 1:7 = $126P_J$ etc.

4.2 Resonant argument and verification of resonance

Whereas Fig. 3 shows many particles, resonant groupings in various a_0 ranges being evident, resonant behaviour is verified by plotting the *resonant argument*, denoted by σ, for individual particles (Fig. 4).

For a 1:7 resonance σ is defined as:

$$\sigma = \lambda_J - 7\lambda + 6\varpi \quad (1)$$

and for a 1:6 resonance (not shown in Fig. 4),

$$\sigma = \lambda_J - 6\lambda + 5\varpi \quad (2)$$

where J is Jupiter and λ, the *mean longitude*, is defined by:

$$\lambda = \varpi + M$$

and ϖ is the *longitude of perihelion*. We define ϖ in relation to a retrograde orbit,

$$\varpi = \Omega - \omega \quad (3)$$

where Ω is longitude of ascending node and ω is argument of perihelion. In the case of a retrograde orbit, ω is subtracted from Ω (Whipple & Shelus 1993; Sekhar & Asher 2014) instead of being added as in the conventional definition of ϖ for a prograde orbit. Equations (1) and (2) for the resonant arguments σ hold because the d'Alembert rules are satisfied (Murray & Dermott 1999, p. 250) (Sekhar & Asher 2014, p. 53). The slowly varying terms (λ_J and λ being rapidly varying) are chosen to be single terms in ϖ because with the particles having high e, these resonances are of the eccentricity type as described in Peale (1976, sec. 2).

Resonant behaviour is identified by verifying that σ librates, or oscillates back and forward within the confines of a single *libration zone* (Emel'yanenko 2001) or *resonant zone* (Kinsman & Asher 2017, sec. 4.20). The above choice of definitions (eq. 1, 2, 3) results, for these 1:6 and 1:7 resonances, in particles librating around the centre of a resonant zone at $\sigma = 0$, the zone's boundaries being at $\sigma = \pm 180°$ (see Fig. 4).

A 1:n resonance divides the 360° mean longitude of the orbit into n resonant zones (Emel'yanenko 2001). So for the 1:7, there are seven resonant zones, yielding a length of ~52° per zone and the centre of each zone would then occur at the centre of that 52° interval (i.e., ±180°/7 = ±26° in λ). Here σ effectively amplifies, by 7 times, the longitude's displacement relative to the resonance centre (cf. eq. 1).

Analogously to the 1:7, the 1:6 orbital ratio produces six zones around the 360° of the orbit, any resonant particle librating within one zone whose total extent is ±30° in M about the respective resonance centre. In the 1:6 or 1:7, each zone of the respectively six or seven zones corresponds to one revolution of Jupiter (~12 yr), i.e. the extent of each zone equalling $\pm\frac{1}{2}P_J$.

4.3 Particles trapped in 1:7 resonance: examples

Figure 4 examines the dynamics of this resonant trapping in detail, i.e., the libration vs circulation of the resonant argument σ corresponding to being trapped in resonance or not. Interestingly enough, even though all four particles are ejected in 911 BC into a 1:7 resonance with Jupiter, two particles closely approach Earth in 417, corresponding to an outburst that year, while the other two particles cause a second outburst in 585. Upper and lower panels show all four particles undergoing resonant librations until 417 and 585 respectively. Whereas most of the particles stay in resonance, indicated by the continuous oscillations, some particles making a close passage to Earth are thrown out of resonance, illustrated in Fig. 4 by a particle exceeding −180° in both 417 and 585.

Table 3 shows the 1:7 resonant returns from the same 911 BC trail in 417 and 585. The osculating semi-major axis a_0 at ejection is smaller for AD 417, ≈ 18.97 au and larger for AD 585, ≈ 19.2 au. Thus two separate initial sizes of the semi-major axis a_0, corresponding to the two separate years

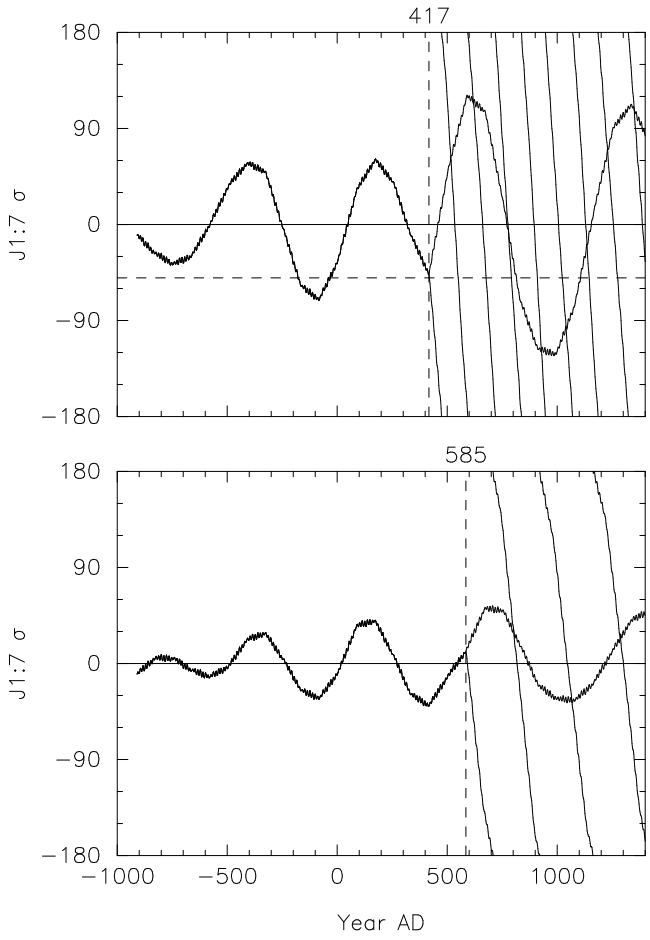

Figure 4. Four particles ejected into the Jovian 1:7 resonance at 1P/Halley's 911 BC perihelion passage. In the upper panel two of these particles, with $\Delta a_0 \approx +1.180$ (Table 1), virtually coincide until 417 when one particle leaves resonance upon approach to Earth. In the lower panel two particles, with $\Delta a_0 \approx +1.343$ (Table 2) are coincidental until 585 when one leaves resonance upon approach to Earth. One particle in each panel continues in resonance indicated by librations within the ±180° boundaries. The libration centre is $\sigma \approx 0°$. Particles out of resonance are indicated by roughly parallel lines extending the full range of −180° to +180°. All four particles show librating resonant argument σ over the whole interval from ejection till Earth approach, as do all other particles from 911 BC contributing to outbursts in both years. The particles in 417 (upper panel) are at $\sigma \approx -50°$ when they approach Earth, somewhat ahead of the libration centre.

417 and 585 when the particles reach Earth, were drawn into the same range of resonant librations about the nominal resonant $a_n = 19.03$ au. The values 18.97 and 19.2 both fall within the quite extensive range of a_0 under the influence of 1:7 (see the main central concentration in Fig. 3).

In fact, Figure 4 shows when the particle is at the front or back of its oscillation as it repeatedly rebounds between ±180°; the resonance centre is $\sigma \approx 0°$ in this case. The sign of σ is arbitrary but with our definition (Eq. 1) positive σ corresponds to particles behind centre and negative σ corresponds to particles ahead of the resonance centre. The initial negative slope shown in the upper panel (Fig. 4) shows forward drift initially where $a < a_n$ while the initial positive slope in the lower panel indicates rearward drift initially where $a > a_n$.

Table 3. Mean motion resonances, Jovian 1:6 and 1:7, causing observable and likely observable outbursts: a_n nominal resonance location (Murray & Dermott 1999, sec. 8.4); a_0 osculating semi-major axis at ejection; Diff = difference in days with recorded event, where + indicates the event followed the probable outburst by the given number of days.

Year	Trail	Reson	a_n	a_0	Obs.	Diff
417 Sep 24	911 BC	1:7	19.03	18.966	Maya	+5
	911 BC	1:7	19.03	18.971	Maya	+5
	911 BC	1:7	19.03	18.974	Maya	+5
585 Sep 23	1266 BC	1:6	17.17	17.447	Maya	+15
	1266 BC	1:6	17.17	17.451	Maya	+15
	1266 BC	1:6	17.17	17.452	Maya	+15
	1266 BC	1:6	17.17	17.454	Maya	+15
	1266 BC	1:6	17.17	17.460	China	0
	1266 BC	1:6	17.17	17.461	China	0
585 Sep 25	911 BC	1:7	19.03	19.238	Maya	+13
	911 BC	1:7	19.03	19.134	Maya	+13

Rendtel (2007) and Arlt et al. (2008) suggest enhanced Orionid activity can reoccur for a few consecutive years. Particles undergoing 1:6 or 1:7 resonant librations can periodically be a few years ahead or behind while remaining in a single resonant zone. Figure 4 shows a Δa_0=+1.180 particle ~1.6 yr forward of the resonance centre in 417 (upper panel: 1.6 yr ahead of centre is $\sigma \approx -50°$ since 360° in σ corresponds to $P_J \approx 11.9$ yr) and a Δa_0=+1.343 particle near the centre in 585 (lower panel). Strictly speaking, regarding the continuous resonance from 911 BC until AD 417, the resonance centre does not reach Earth until 419, which is 112 (= 16 × 7) P_J after 911 BC. Thus precisely, 419 and 585 are separated by 2 resonant revolutions = $14P_J$. In practice, however, 417 and 419 are within the same resonant zone, particles in 417 September reaching the ascending node ~1.6 yr (~50° in σ) before those at the resonance centre do so.[3]

4.4 The year AD 585, the 1266 BC trail and returns from 1:6 resonance

The 585 outbursts on September 23rd were due to a 1:6 Jovian resonance of particles released at the 1266 BC passage of 1P/Halley (librating σ plots analogous to Fig. 4 confirmed but not shown here). Table 2 gives the parameters of the 585 outbursts and Table 3 shows the details of the mean motion resonance. As noted in Section 3, the outbursts from the 1266 BC trail with $a_0 \approx 17.45$ au, where the nominal $a_n = 17.17$ au, were visible both to the Maya and the Chinese. Contrary to the earlier situation describing the 417 outburst ~1.6 yr prior to the 419 resonance centre (Sec. 4.3),

[3] It is not the purpose of this paper to present details of the locations of resonant zones, such as listing perihelion passage times of the centres of these zones, but as we refer to these times in a few cases, we note that they can be computed by constructing diagrams as in Sekhar & Asher (2014, p.54). Sekhar has made corresponding computations for resonances in other streams (Sekhar 2014), resonances with other planets (Sekhar & Asher 2013) and three body resonances (Sekhar et al. 2016).

AD 585 was right on the 1:6 resonance centre from the 1266 BC ejection, i.e., 26 revolutions at 1:6 (156 P_J).

Since Comet Halley was 1:6 resonant from 1404 BC to 690 BC (Sekhar & Asher 2014, p. 53), any particles ejected in that interval have an increased chance of being locked in the same 1:6 resonance. In fact, typical meteoroid ejection speeds are large enough to bring other resonances like 1:7 within range too (cf. Fig. 3). Moreover during that interval the returns when Halley is nearest the 1:6 resonance centre are particularly favourable for populating 1:n resonances; 911 BC is best, followed by 1266 BC, then 1198 BC, then 986 BC. This is supported by computations of present epoch outbursts from trails created at these favourable returns (Sato & Watanabe 2007, table 1) (Sekhar & Asher 2014, table 1). In actuality, Comet Halley was very close to the 1:6 resonance centre at its 911 BC return (particles starting only slightly below zero in Fig. 4).

5 CONCLUSIONS

The authors have presented evidence that there was a high probability of Orionid outbursts occurring in the years 417 and 585. Particles trapped in resonance from Comet Halley's perihelion passages in 1266 BC and 911 BC would have provided sharp, dense and well-defined displays under near ideal conditions for the Maya. The authors confirmed the Chinese observation in 585, verified by particles from the 1266 BC Comet Halley trail resonant with Jupiter in a 1:6 orbital ratio. Further, in a rather unusual display of orbital gymnastics, this same tightly packed stream segment that caused the China outburst would only hours earlier have caused a dramatic display visible to Maya observers. Although the Orionids have been an annual meteor shower since at least AD 288 (Pankenier et al. 2008)(p. 309), (Zhuang 1977)(entry 100, p. 205), (Hasegawa 1993)(entry 160, p. 215), actual outbursts prior to the year 900 seem to have been a rarity as evidenced by only two recorded observations by China.

ACKNOWLEDGEMENTS

Plots used Prof. Timothy J. Pearson's excellent PGPLOT subroutine library. Astronomy at Armagh is supported by the N. Ireland Dept. for Communities. The authors are very grateful to the editor and reviewers; their comments were responsible for a significant improvement in our paper.

REFERENCES

Adams R. E. W., 1999, Rio Azul: An Ancient Maya City. University of Oklahoma Press, Norman
Aldana G., 2005, Ancient Mesoamerica, 16, 305
Arlt R., Brown P., 1999, WGN, J. Int. Meteor Organization, 27, 267
Arlt R., Bellot Rubio L., Brown P., Gyssens M., 1999, WGN, J. Int. Meteor Organization, 27, 286
Arlt R., Rendtel J., Bader P., 2008, WGN, J. Int. Meteor Organization, 36, 55
Asher D. J., 2000, in Arlt R., ed., Proc. Int. Meteor Conf., Frasso Sabino 1999. Int. Meteor Organization, pp 5–21
Asher D. J., Clube S. V. M., 1993, QJRAS, 34, 481
Asher D. J., Emel'yanenko V. V., 2002, MNRAS, 331, 126
Chambers J. E., 1999, MNRAS, 304, 793
Egal A., Wiegert P., Brown P. G., Moser D. E., Campbell-Brown M., Moorhead A., Ehlert S., Moticska N., 2019, Icarus, 330, 123
Emel'yanenko V. V., 2001, in Warmbein B., ed., ESA SP Vol. 495, Proc. Meteoroids 2001 Conf. ESA, Noordwijk, pp 43–45
Emel'yanenko V. V., Bailey M. E., 1996, in Gustafson B. A. S., Hanner M. S., eds, ASP Conf. Ser. Vol. 104, Physics, Chemistry and Dynamics of Interplanetary Dust. Astron. Soc. Pac., San Francisco, pp 121–124
Everhart E., 1985, in Carusi A., Valsecchi G. B., eds, Astrophys. Space Sci. Libr. Vol. 115, Proc. IAU Colloq. 83, Dynamics of Comets: Their Origin and Evolution. Reidel, Dordrecht, pp 185–202
Froeschlé C., Froeschlé C., 1992, Celest. Mech. Dyn. Astron., 54, 71
Froeschlé C., Scholl H., 1986, A&A, 158, 259
Giorgini J. D., et al., 1996, BAAS, 28, 1158
Grube N., Martin S., 2004, in Notebook for the XXVIIIth Maya Hieroglyphic Forum at Texas, March 2004. Maya Workshop Foundation, The University of Texas at Austin, pp II.1–II.95
Hasegawa I., 1993, in Štohl J., Williams I. P., eds, Meteoroids and their Parent Bodies. Astron. Inst., Slovak Acad. Sci., Bratislava, pp 209–223
Helmke C., Awe J. J., 2016, The PARI Journal, 16(4), 1
Jenniskens P., et al., 2002, Icarus, 159, 197
Kennett D. J., et al., 2013, Sci. Rep., 3, 1597
Kinsman J. H., Asher D. J., 2017, Planet. Space Sci., 144, 112
Martin S., 2015, The PARI Journal, 15(3), 1
Martin S., Skidmore J., 2012, The PARI Journal, 13(2), 3
Mathews P., 2006,2009,2014, The Maya Dates Project. In progress and unpublished. La Trobe University, Melbourne
McNaught R. H., Asher D. J., 1999, WGN, J. Int. Meteor Organization, 27, 85
Morley F. R., Morley S. G., 1938, Contrib. Amer. Anthropol. Hist., 5 (No. 24), 1
Murray C. D., Dermott S. F., 1999, Solar System Dynamics. Cambridge University Press
Pankenier D. W., Xu Z., Jiang Y., 2008, Archaeoastronomy in East Asia: Historical Observational Records of Comets and Meteor Showers from China, Japan, and Korea. Cambria Press, Amherst, New York
Peale S. J., 1976, ARA&A, 14, 215
Plavec M., 1956, Vistas Astron., 2, 994
Plavec M., 1957, Publ. Astron. Inst. Czechosl. Acad. Sci., 30, 1
Prager C., Gronemeyer S., Wagner E., Matsumoto M., Kiel N., 2014, A Checklist of Archaeological Sites with Hieroglyphic Inscriptions, https://mayawoerterbuch.de
Rendtel J., 2007, WGN, J. Int. Meteor Organization, 35, 41
Ryabova G. O., 2003, MNRAS, 341, 739
Sato M., Watanabe J., 2007, PASJ, 59, L21
Sato M., Watanabe J.-i., Tsuchiya C., Moorhead A. V., Moser D. E., Brown P. G., Cooke W. J., 2017, Planet. Space Sci., 143, 132
Schele L., Freidel D., 1990, A Forest of Kings: The Untold Story of the Ancient Maya. William Morrow and Company, Inc., New York
Schele L., Miller M. E., 1986, The Blood of Kings: Dynasty and Ritual in Maya Art. Kimbell Art Museum, Fort Worth
Scholl H., Froeschlé C., 1988, A&A, 195, 345
Sekhar A., 2014, PhD thesis, Queen's University Belfast, doi:10.5281/zenodo.55994
Sekhar A., Asher D. J., 2013, MNRAS, 433, L84
Sekhar A., Asher D. J., 2014, Meteorit. Planet. Sci., 49, 52
Sekhar A., Asher D. J., Vaubaillon J., 2016, MNRAS, 460, 1417
Stuart D., 2004, The Entering of the Day: An Unusual Date from Northern Campeche, www.mesoweb.com/stuart/notes/EnteringDay.pdf

Stuart D., Canuto M., 2017, in Maya Hieroglyph Workshop, January 10–11, 2017. University of Texas at Austin
Stuart D., Canuto M., Barrientos Quezada T., Lamoureax St-Hillaire M., 2015, Preliminary Notes on Two Recently Discovered Inscriptions from La Corona, Guatemala, https://mayadecipherment.com
Trigo-Rodríguez J. M., Madiedo J. M., Llorca J., Gural P. S., Pujols P., Tezel T., 2007, MNRAS, 380, 126
Vail G., Hernández C., 2018, The Maya Codices Database, version 5.0, http://www.mayacodices.org
Vaubaillon J., Neslušan L., Sekhar A., Rudawska R., Ryabova G. O., 2019, in Ryabova G. O., Asher D. J., Campbell-Brown M. D., eds, Meteoroids: Sources of Meteors on Earth and Beyond. Cambridge University Press, pp 161–186
Whipple A. L., Shelus P. J., 1993, Icarus, 101, 265
Wiegert P., Vaubaillon J., Campbell-Brown M., 2009, Icarus, 201, 295
Yeomans D. K., Kiang T., 1981, MNRAS, 197, 633
Zhuang T. S., 1977, Chinese Astron., 1, 197

APPENDIX A: DATA BASE OF MAYA CLASSIC PERIOD DATES INTEGRATED FOR POSSIBLE ORIONID OUTBURSTS

This paper has been typeset from a TEX/LATEX file prepared by the author.

Table A1. ORI Data Set. Columns: Julian Calendar Date (Martin & Skidmore 2012), J2000 Solar Longitude; location, site where the date is inscribed. *1 refers to a portable object (see Morley & Morley 1938). *27 refers to one of four extant painted screeenfold books. As a matter of note, one event known as a 'Star' War was recorded on 692 Oct 5, within the possible time frame of the Orionids. 'Star War' refers to a war event that is denoted by a hieroglyph containing the sign for 'star,' known as the 'star-over-earth' hieroglyph. In his publication about the 'Star War' hieroglyph, Aldana (2005) proposes a connection between sporadic meteors and the Star War event through purely historical reassessment and a 'coordinate free' environment (i.e., no correlation constant) and therefore unfortunately no correlations to specific dates can be determined; he discounts meteor showers because 'Modern science's ability to calculate this variation becomes increasingly suspect the farther it projects into the past, making reconstructions for the Classic period unreliable' (Aldana 2005, p.314). Sporadic meteors are those meteors which are unrelated to established meteor showers. Although it is possible that 'star-over-earth' does refer to sporadic meteors, it is nearly impossible to prove at this juncture and furthermore sporadic meteors are very common (Wiegert et al. 2009). Meteor outburst predictions however, have proven to be very accurate using computerized orbital integrations (Arlt et al. 1999; Sato et al. 2017; Egal et al. 2019; Vaubaillon et al. 2019) both with recent orbital revolutions and in particular regarding resonances produced over centuries (Arlt & Brown 1999; Asher & Emel'yanenko 2002; Rendtel 2007; Sato & Watanabe 2007; Trigo-Rodríguez et al. 2007). The correlation constant of 584286 (actually the base date of the Maya calendar in terms of the Julian Day Number) is a virtual certainty using the Martin & Skidmore (2012) argument and the most recent high precision radiocarbon dating (Kennett et al. 2013). Using this correlation constant the authors produce the specific dates in this table, however, only one out of 30 associated events contained the 'Star War' hieroglyph, a date with a year (692) in which the authors found no Orionid outburst.

	Date Julian	Solar Long	Location
*1	320 Sep 17	198.°445	Artifact* (coastal Guatemala)
2	378 Oct 7	217.°531	Yaxchilan, Chiapas, Mexico
3	402 Sep 28	208.°369	Yaxchilan, Chiapas, Mexico
4	417 Sep 29	209.°519	Rio Azul, Peten, Guatemala
5	508 Sep 25	205.°196	Palenque, Chiapas, Mexico
6	524 Sep 19	199.°126	Palenque, Chiapas, Mexico
7	557 Sep 16	195.°694	Tikal, Peten, Guatemala
8	585 Oct 8	217.°435	Naranjo, Peten, Guatemala
9	614 Sep 23	202.°022	Bonampak, Chiapas, Mexico
10	625 Sep 30	209.°171	La Corona, Peten, Guatemala
11	629 Oct 2	211.°147	Caracol, Belize
12	630 Oct 2	210.°885	Naranjo, Peten, Guatemala
13	634 Sep 28	206.°874	Caracol, Belize
14	638 Sep 20	198.°892	Caracol, Belize
15	640 Sep 25	204.°347	Caracol, Belize
16	649 Sep 25	204.°035	Palenque, Chiapas, Mexico
17	664 Oct 1	210.°176	La Corona, Peten, Guatemala
18	667 Sep 20	198.°456	La Corona, Peten, Guatemala
19	675 Sep 22	200.°392	La Corona, Peten, Guatemala
20	689 Sep 26	204.°774	La Corona, Peten, Guatemala
21	692 Oct 5	213.°983	Tonina, Chiapas, Mexico
22	714 Sep 24	202.°380	Naranjo, Peten, Guatemala
23	724 Sep 24	202.°810	Palenque, Chiapas, Mexico
24	735 Sep 23	201.°005	Tikal, Peten, Guatemala
25	767 Sep 24	201.°790	Itzan, Peten, Guatemala
26	773 Sep 23	201.°254	Copan, (western) Honduras
*27	775 Sep 30	207.°711	Dresden Codex*
28	836 Sep 24	202.°094	Hecelchakan, Campeche, Mexico
29	859 Oct 6	213.°162	Caracol, Belize
30	874 Sep 28	205.°334	Seibal, Peten, Guatemala